International Journal of Nanomedicine

Dovepress
open access to scientific and medical research

Open Access Full Text Article

ORIGINAL RESEARCH

Combined Placental Mesenchymal Stem Cells with Guided Nanoparticles Effective Against Diabetic Nephropathy in Mouse Model

Ke Wang[1,2,*], Te Liu[1,*], Yucheng Zhang[1], Huiying Lv[1], Hua Yao[1], Ye Zhao[3], Jing Li[1], Xiuying Li[1]

[1]Scientific Research Center, China-Japan Union Hospital of Jilin University, Changchun, Jilin, People's Republic of China; [2]Gynecology and Obstetrics Department, China-Japan Union Hospital of Jilin University, Changchun, Jilin, People's Republic of China; [3]Dermatological Department, China-Japan Union Hospital of Jilin University, Changchun, Jilin, People's Republic of China

*These authors contributed equally to this work

Correspondence: Xiuying Li; Jing Li, Email lixiuying@jlu.edu.cn; lijing1029@jlu.edu.cn

Background: Diabetic nephropathy (DN) is a prevalent complication of diabetes mellitus and constitutes the primary cause of mortality in affected patients. Previous studies have shown that placental mesenchymal stem cells (PL-MSCs) can alleviate kidney dysfunction in animal models of DN. However, the limited ability of mesenchymal stem cells (MSCs) to home to damaged sites restricts their therapeutic potential. Enhancing the precision of PL-MSCs' homing to target tissues is therefore vital for the success of cell therapies in treating DN.

Methods: We developed Fe_3O_4 coated polydopamine nanoparticle (NP)-internalized MSCs and evaluated their therapeutic effectiveness in a mouse model of streptozotocin- and high-fat diet-induced DN, using an external magnetic field.

Results: Our study confirmed that NPs were effectively internalized into PL-MSCs without compromising their intrinsic stem cell properties. The magnetic targeting of PL-MSCs notably improved their homing to the kidney tissues in mice with DN, resulting in enhanced kidney function compared to the transplantation of PL-MSCs alone. Furthermore, the anti-inflammatory and antifibrotic attributes of PL-MSCs played a role in the recovery of kidney function and structure.

Conclusion: These results demonstrate that magnetically targeted therapy using PL-MSCs is a promising approach for treating diabetic nephropathy.

Keywords: diabetic nephropathy, magnetic targeting, mesenchymal stem cells, iron oxide nanoparticles

Introduction

Diabetes is among the most prevalent diseases globally, and its incidence continues to rise. The complications associated with type 2 diabetes, along with the adverse reactions to antidiabetic treatments, significantly affect patients' quality of life and pose direct health risks.[1] Therefore, preventing and delaying diabetes-related complications are essential clinical objectives.[2,3] Diabetic nephropathy (DN), a primary chronic microvascular complication of diabetes, is a leading cause of end-stage renal disease.[4] Once DN progresses to end-stage kidney disease, its complex metabolic characteristics render it more challenging to treat compared to other kidney diseases. DN's key pathological features include glomerular sclerosis, thickening of the basement membrane, and mesangial dilation. Other features are apoptosis and loss of podocytes, renal interstitial inflammatory infiltration, and fibrosis.[5] Although drugs that lower blood sugar or blood pressure, along with angiotensin inhibitors, can delay the onset of DN, they cannot completely prevent it.[6] Presently, there is no cure for DN, making the exploration of novel, DN-specific treatment strategies imperative.

Stem cell therapy represents an innovative approach for treating various diseases, potentially outperforming single-agent drug therapies.[7] Increasing evidence indicates that mesenchymal stem cells (MSCs) not only improve renal function[8] but also prevent the progression of DN[9,10] and reduce overt albuminuria.[11,12] Placental MSCs (PL-MSCs) are particularly promising

Received: 26 October 2023
Accepted: 13 January 2024
Published: 26 January 2024

due to their higher proliferation potential, differentiation capabilities, and lower immunogenicity compared to MSCs from other tissues.[13] For effective treatment, it is crucial to achieve efficient homing of MSCs to damaged tissues.[11] Generally administered intravenously, MSCs often show low uptake at injury sites, suggesting that enhancing their targeted homing capability could be a novel strategy to improve DN treatment efficacy.

Magnetic targeting systems using magnetically labeled cells have proven more effective in cell delivery to injury sites than non-magnetic systems.[14,15] Recent studies demonstrate that external magnets can effectively guide magnetically labeled cells to specific locations in vivo, a process known as magnetic cell attraction.[16] Superparamagnetic iron oxide nanoparticles (NPs) are ideal for this purpose, attaching to and being internalized by MSC surfaces. These NPs serve as efficient tracers for MSCs, with labeling efficiencies > 90% without transfection agents.[17,18] Due to their biocompatibility and responsiveness to external magnetic fields, NPs are invaluable in advanced biomedical applications, including MRI cell tracking, drug delivery, and magnetic cell attraction.

In this study, we developed a novel type of NP-labeled PL-MSCs and employed a magnetic targeting delivery approach to direct their migration to the kidneys. We also assessed the therapeutic effects of these NP-labeled MSCs in a mouse model of DN.

Materials and Methods

The Separation and Identification of Placental Mesenchymal Stem Cells (PL-MSCs)

MSCs were isolated from human placentas following normal cesarean births and cultured according to previously described methods.[13] Written informed consent was obtained from all participants, and the study received approval from the Ethics Committee of the China-Japan Union Hospital of Jilin University. The PL-MSCs were cultured in osteogenic and adipogenic differentiation media (StemPro® Osteogenesis Differentiation kit; Invitrogen Australia Pty Ltd.) for 28 and 21 days, respectively. Subsequently, they were stained with Alizarin Red S for osteogenic differentiation and Oil Red O for adipogenic differentiation. Key cell surface markers, including CD73, CD45, CD34, and CD105 (Beckman, USA), were identified using flow cytometry (FACScan; BD Biosciences).

Synthesis and Characterization of Fe_3O_4 Coated with Polydopamine Nanoparticles

Fe_3O_4 coated with Polydopamine (Fe_3O_4@PDA) NPs were synthesized following the method previously described.[14] The synthesized NPs were examined using an H-800 transmission electron microscope (Hitachi Ltd., Tokyo, Japan). Additionally, the hydrodynamic size of the NPs was determined using NanoSight Nanoparticle Tracking Analysis (NTA) 3.1.

Internalization of Fe_3O_4 Coated with Polydopamine Nanoparticles by PL-MSCs

Third-passage PL-MSCs were seeded at a density of 3×10^5 cells per well in a six-well plate, using 2 mL of complete medium, and incubated under standard conditions for 24 h. Various concentrations of NPs (0, 25, 50, 100, 150, and 200 μg/mL) were added to the medium and incubated for an additional 24 h. Post-incubation, the wells were thoroughly washed with warm, sterile phosphate-buffered saline (PBS) to eliminate any residual NPs.

Detection of Intracellular Iron via Prussian Blue Staining

To detect iron particles within the labeled PL-MSCs, Prussian blue staining was employed. Initially, the cells were fixed in 4% paraformaldehyde for 30 min and subsequently washed three times with PBS. After fixation, the cells were stained with Prussian blue staining solution (Beijing Solarbio Science and Technology Co. Ltd., Beijing, China) for 30 min. Following staining, the cells were thoroughly rinsed with water and examined under a microscope (CKX 41; Olympus, Japan).

Detection of Intracellular Iron with Inductively Coupled Plasma-Optical Emission Spectroscopy

To measure intracellular iron content, we utilized the PerkinElmer Optima 3300DV system (PerkinElmer Inc., Waltham, MA, USA) employing Coupled Plasma-Optical Emission Spectroscopy (ICP-OES).

Detection of Intracellular Iron with Transmission Electron Microscopy

The kidney tissues and PL-MSCs labeled with NPs at a concentration of 50 μg/mL, were fixed in 2.5% glutaraldehyde for 24 h at 4 °C. Following fixation, the samples were washed with PBS and then post-fixed with 1% osmium tetroxide for 2 h. After undergoing dehydration in graded ethanol solutions, the tissue and cell samples were prepared for examination using Transmission electron microscopy (TEM)(HITACHI, HT7800, Japan).

Assessment of Nanoparticle Cytotoxicity

The PL-MSCs were exposed to various concentrations (0, 25, 50, 100, 150, and 200 μg/mL) of NPs. A Cell Counting Kit-8 (CCK8) assay (KeyGEN BioTECH, Nanjing, China) was conducted to assess cell viability and proliferation following the manufacturer's instructions. The NP concentration demonstrating the lowest cytotoxicity was selected for further in vitro and in vivo studies.

To evaluate whether NPs induce aging in MSCs, a soluble β-galactosidase assay was performed as previously described.[14] Briefly, MSCs were plated in six-well plates at a density of 3×10^5 cells per well. After 12 h, the medium was removed, and the MSCs were incubated with varying NP concentrations (0, 25, 50, 100, 150, and 200 μg/mL) in 2 mL of medium for 24 h. The cells were then lysed through repeated freeze/thaw cycles. The supernatants were collected for β-galactosidase analysis using a human β-galactosidase ELISA kit (Molbio, Shanghai, China), in accordance with the manufacturer's protocol. Absorbance was measured at 450 nm using a microplate reader (Bio-Rad Laboratories Inc., Hercules, CA, USA).

Animals

C57BL/6J mice, aged 5 weeks, were acquired from Beijing Weitong Lihua Experimental Animal Technology Co. Ltd., China. All in vivo animal experiments received approval from the Jilin University Animal Welfare and Research Ethics Committee. These experiments were conducted in accordance with the "Guidelines for the Ethical Review of Laboratory Animal Welfare (GB/T 35892–2018)."

Induction of Diabetic Nephropathy in Mouse Model and Outline of Experimental Protocols

Mice were acclimatized for one week before being placed on a high-fat diet (HFD, Beijing HFK Bioscience Co., Ltd, China, No.12492), which consisted of 60% fat, modified by the addition of 3.2% soybean oil, and was provided ad libitum for eight weeks. The mice on this diet were then intraperitoneally injected with streptozotocin (STZ) (dissolved in sodium citrate, pH 4.5) at a dosage of 30 mg/kg body weight per day for five consecutive days to induce diabetes (Figure 1). One week later, blood samples were taken from each mouse's tail vein for five consecutive days. Mice exhibiting hyperglycemia (blood glucose levels ≥11.1 mmol/L) were identified as successful models of diabetes.[19]

After developing diabetes, the mice continued on the HFD for an additional 12 weeks and were then randomly divided into five groups, each containing 10 mice: a normal control group (normal), a PBS-treated group (PBS), an MSC-treated group (MSC), an MSC + NPs group (MSCs labeled with NPs, MSC-NP), and a magnetically targeted MSC group (MSCs labeled with NPs and directed using a magnetic field, MSC-NP-MAG). PL-MSCs or PL-MSCs labeled with NPs (5×10^5) were resuspended in 0.2 mL of PBS and administered intravenously via the tail vein. In the MSC-NP-MAG group, after the injection of NP-labeled MSCs, a magnet (1.2 T) was positioned under the kidney area for 20 min (Figure 1). At the end of the experiment, all mice were euthanized for the collection of kidney tissue, urine, and blood samples.

Physiological and Biochemical Analysis

Measurements of water intake, body weight, kidney weight, and blood glucose levels were conducted. Urine samples were collected for the determination of urine creatinine levels. Similarly, blood samples were analyzed to assess serum creatinine and blood urea nitrogen levels, using detection kits (Nanjing Jiancheng Bioengineering Institute, Nanjing, China). Additionally, microalbuminuria levels in urine were quantified using a mouse microalbuminuria ELISA kit (Mlbio, Shanghai, China).

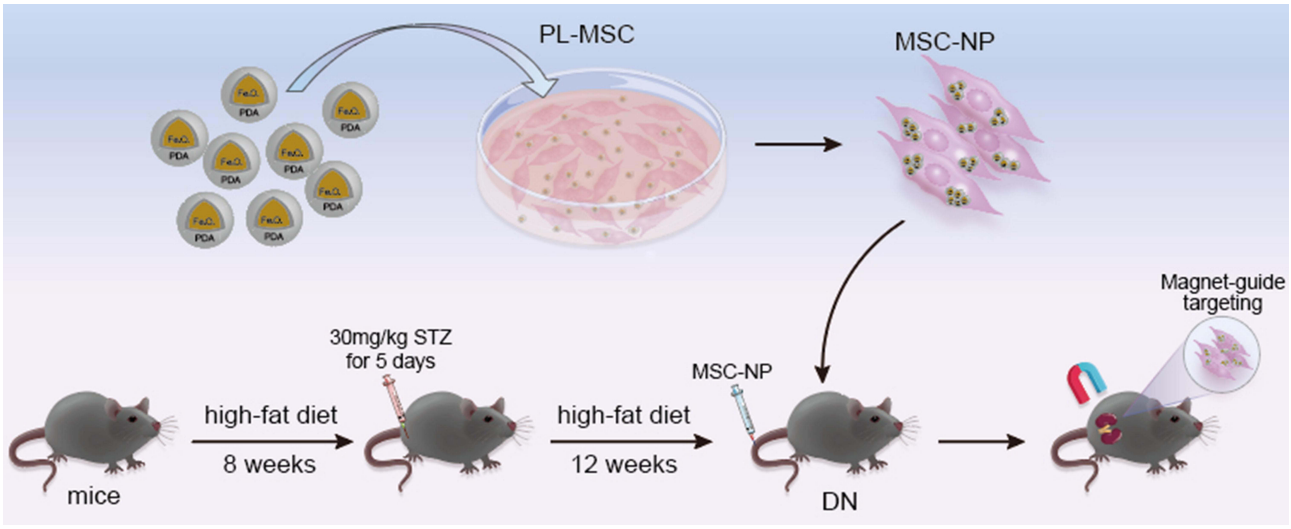

Figure 1 Schematic Overview of the Entire Experiment.

Histological Analysis, Immunohistochemistry, and Immunofluorescence Staining

Kidney tissues were fixed in 4% polyformaldehyde, embedded in paraffin, and sectioned. The sections were stained with Hematoxylin and Eosin (H&E) for general histology. To assess pathological damage and fibrosis, sections were stained with Periodic Acid-Schiff (PAS) and Masson's Trichrome (MT), respectively. The stained slices were then scanned using the Panoramic SCAN (3DHISTECH Ltd, Budapest, Hungary).

For immunohistochemistry, the sections were incubated overnight at 4 °C with primary antibodies: rabbit anti-α-smooth muscle actin (α-SMA) (1:3000, Proteintech, Wuhan, China), rabbit anti-transforming growth factor (TGF)-β (1:200, Boster, Wuhan, China), and mouse anti-MAB1281 (1:200, EMD Millipore, MA, USA). This was followed by the addition of a goat anti-rabbit IgG secondary antibody with horseradish peroxidase labeling (Boster). After washing with PBS, the sections were exposed to 3, 3'-diaminobenzidine for 30 min to visualize the proteins. The stained sections were photographed using the Nikon ECLIPSE Ci upright microscope (Nikon, Japan).

For immunofluorescence staining, kidney paraffin sections were incubated overnight at 4 °C with rabbit anti-F4/80 (1:200, Abcam, Cambridge, UK), rabbit anti-CD3 (1:200, Bioss, China), and rabbit anti-collagen IV antibodies (1:100, Abcam). After a PBS wash, corresponding secondary antibodies (Boster) were applied and incubated at room temperature (24 °C) for 60 min in the dark. Finally, 4', 6-diamidino-2-phenylindole (DAPI) staining (Beyotime, Shanghai, China) was performed, and images were captured using a fluorescence microscope (BX 53; Olympus, Japan).

Serum Cytokine Profile Analysis

The Luminex assay was utilized to quantify cytokines in serum samples. These included interleukin (IL)-1β, IL-2, IL-4, IL-6, IL-10, IL-12, tumor necrosis factor (TNF)-α, and interferon (IFN)-γ. This analysis was conducted in accordance with the manufacturer's protocol and as previously described.[14] Data analysis was performed using the Milliplex Array V5.1 software (Luminex Corporation, Austin, TX, USA).

RNA Extraction and Quantitative PCR Assay

Total RNA was extracted from kidney tissues using TRIzol reagent (Life Technologies, CA, USA). The reverse transcription process followed the protocol provided by TaKaRa (Osaka, Japan). Subsequently, Reverse Transcription-Polymerase Chain Reaction (RT-PCR) was carried out using a StepOnePlus Quantitative PCR (qPCR) System (Applied Biosystems, Warrington, UK). Primers were custom-designed and synthesized by Sangon Biotechnology (Shanghai, China). The specific sequences of these primers for qPCR are detailed in Table 1. Each sample was analyzed in triplicate, and the relative expression levels were determined using the comparative $2^{-\Delta\Delta CT}$ method.

Table 1 Gene-Specific Forward and Reverse Primer Sequence

Gene	Direction	Primer Sequences
β-Actin	Forward	CACCCGCGAGTACAACCTTC
	Reverse	CCCATACCCACCATCACACC
IL-1β	Forward	CTCGCAGCAGCACATCAACAAG
	Reverse	CCACGGGAAAGACACAGGTAGC
IL-6	Forward	TTCTTGGGACTGATGCTGGTGAC
	Reverse	CTGTTGGGAGTGGTATCCTCTGTG
TGF-β	Forward	GGGCATCGCTCATCTCCACAG
	Reverse	GCAACAGGTCAAGTCGTTCTTCAC
TNF-α	Forward	CCACCACGCTCTTCTGTCTACTG
	Reverse	TGGTTTGTGAGTGTGAGGGTCTG
IL-4	Forward	F-ATGGATGTGCCAAACGTCCT
	Reverse	R-AAGCACCTTGGAAGCCCTAC
IL-2	Forward	GACCTCTGCGGCATGTTCTGG
	Reverse	GTCCACCACAGTTGCTGACTCATC
IL-10	Forward	TGGACAACATACTGCTAACCGACTC
	Reverse	AGCCGCATCCTGAGGGTCTTC
IL-12	Forward	GCCAGGGACCAGCAAACACATC
	Reverse	TTCTCAACGCAGCAGCCATCAC
IFN-γ	Forward	CTGGAGGAACTGGCAAAAGGATGG
	Reverse	TCGCCTTGCTGTTGCTGAAGAAG

Statistical Analysis

Data are presented as mean ± standard error of the mean (SEM). Statistical analyses were conducted using SPSS software (version 22.0; Chicago, IL, USA). Group comparisons were made using analysis of variance (ANOVA), followed by Bonferroni post hoc tests for multiple comparisons. $P < 0.05$ was considered statistically significant.

Results and Discussion

We investigated the effect of NP concentration on MSC labeling by incubating MSCs with varying NP concentrations for 24 h. At a concentration as low as 25 μg/mL, nearly 100% of MSCs tested positive for Prussian blue staining, indicating NP internalization. Notably, the Prussian blue intensity increased in proportion to the NP concentration (Figure 2A).

Our findings suggest that NPs are efficiently incorporated into target cells, and the extent of incorporation depends on the NP concentration in the culture medium. We quantified the cellular uptake of NPs by measuring the iron content in cells incubated with NP concentrations ranging from 25 to 200 μg/mL for 24 h. Consistent with the Prussian blue results, cellular iron content increased with higher NP concentrations in the medium (Figure 2B). We successfully labeled MSCs with up to 26.1 ± 1.0 pg of iron per cell. In summary, NPs in the culture medium effectively and efficiently label MSCs.

Cell viability and proliferation ability are critical for the success of cell therapy and tissue engineering.[20–22] We evaluated NP toxicity by incubating PL-MSCs with different NP concentrations for 24 h. No cytotoxicity was observed at NP concentrations of 25 or 50 μg/mL. However, concentrations of 150 and 200 μg/mL induced cytotoxicity (Figure 2C). β-Galactosidase levels significantly increased at NP concentrations of 150 and 200 μg/mL but remained unchanged below 100 μg/mL (Figure 2D). According to the CCK8 assay, cell proliferation was not significantly affected at NP concentrations of 25 and 50 μg/mL. However, concentrations above 100 μg/mL reduced proliferative capacity, possibly due to iron oxide toxicity and the generation of free radicals through the Fenton reaction.[23] Degradation of NPs in acidic endosomal/lysosomal environments releases free iron into the cytoplasm, which oxidizes to iron oxide.[24] These observations suggest that an NP concentration of 50 μg/mL is optimal for the growth and proliferation of PL-MSCs, and was thus selected for further studies.

To determine if endocytosis was the mechanism for NP entry into the cytoplasm, we used TEM to locate NPs within the cells. Most NPs were found inside endosome-like structures in the cytoplasm (Figure 2F and G), with none detected

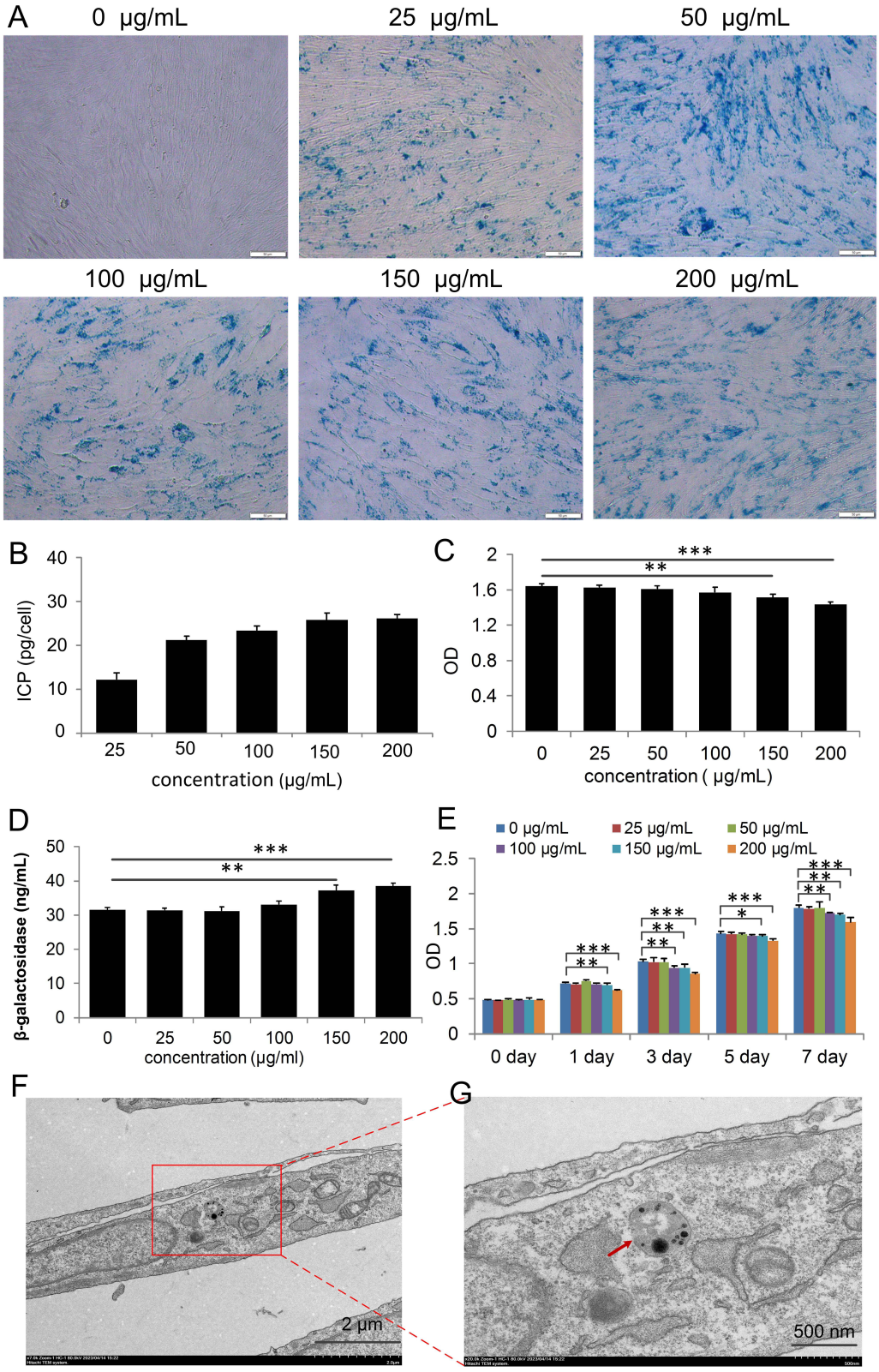

Figure 2 Internalization of Nanoparticles (NPs) into Placental Mesenchymal Stem Cells (PL-MSCs). (**A**) MSCs stained with Prussian Blue to highlight iron (Fe) content. Scale bar = 50 μm. (**B**) Quantification of Fe concentration using Inductively Coupled Plasma-Optical Emission Spectroscopy (ICP-OES) (n=3). (**C**) Assessment of NP-induced cytotoxicity in MSCs labeled with NPs at varying concentrations for 24 h (n=4). (**D**) Measurement of β-galactosidase levels in NP-labeled MSCs using ELISA (n=4). (**E**) Proliferation rates of cells labeled with NPs at different concentrations (n=5). (**F** and **G**) Transmission Electron Microscopy (TEM) images showing NPs internalized into an MSC at a concentration of 50 μg/mL. The red arrow indicates NP. Data are presented as mean ± S.E.M. *P*-values < 0.05 were considered statistically significant, denoted as **P* < 0.05; ***P* < 0.01; ****P* < 0.001.

in the nucleus of MSCs. To determine the impact of NPs on the essential characteristics of MSCs, we assessed these characteristics in the MSC+NP group using the minimal criteria defined for MSCs.[25] Flow cytometry analysis revealed strong positive expression of surface markers CD73 and CD105 in PL-MSCs, while hematopoietic progenitor markers CD34 and CD45 were absent (Figure 3A). This indicates that NP labeling did not alter the immunophenotype of the PL-MSCs. MSCs are multipotent cells capable of differentiating into various lineages such as osteocytes, chondrocytes, and adipocytes.[26,27] We observed that both untreated MSCs and NP-MSCs exhibited similar differentiation capabilities (Figure 3B). Overall, our findings suggest that 50 μg/mL NPs do not compromise the fundamental characteristics of these stem cells.

Figure 4 illustrates significant increases in various renal functional parameters, including water intake (Figure 4A), kidney weight (Figure 4D), kidney index (Figure 4E), serum urea nitrogen (Figure 4F), serum creatinine (Figure 4G), urine creatinine (Figure 4H), and urinary albumin (Figure 4I), in the DN group compared to the normal group. In contrast, these parameters were notably reduced in the PL-MSC-treated group. Notably, this reduction was more pronounced in the group receiving magnetically targeted PL-MSC transplantation than in the group treated with PL-

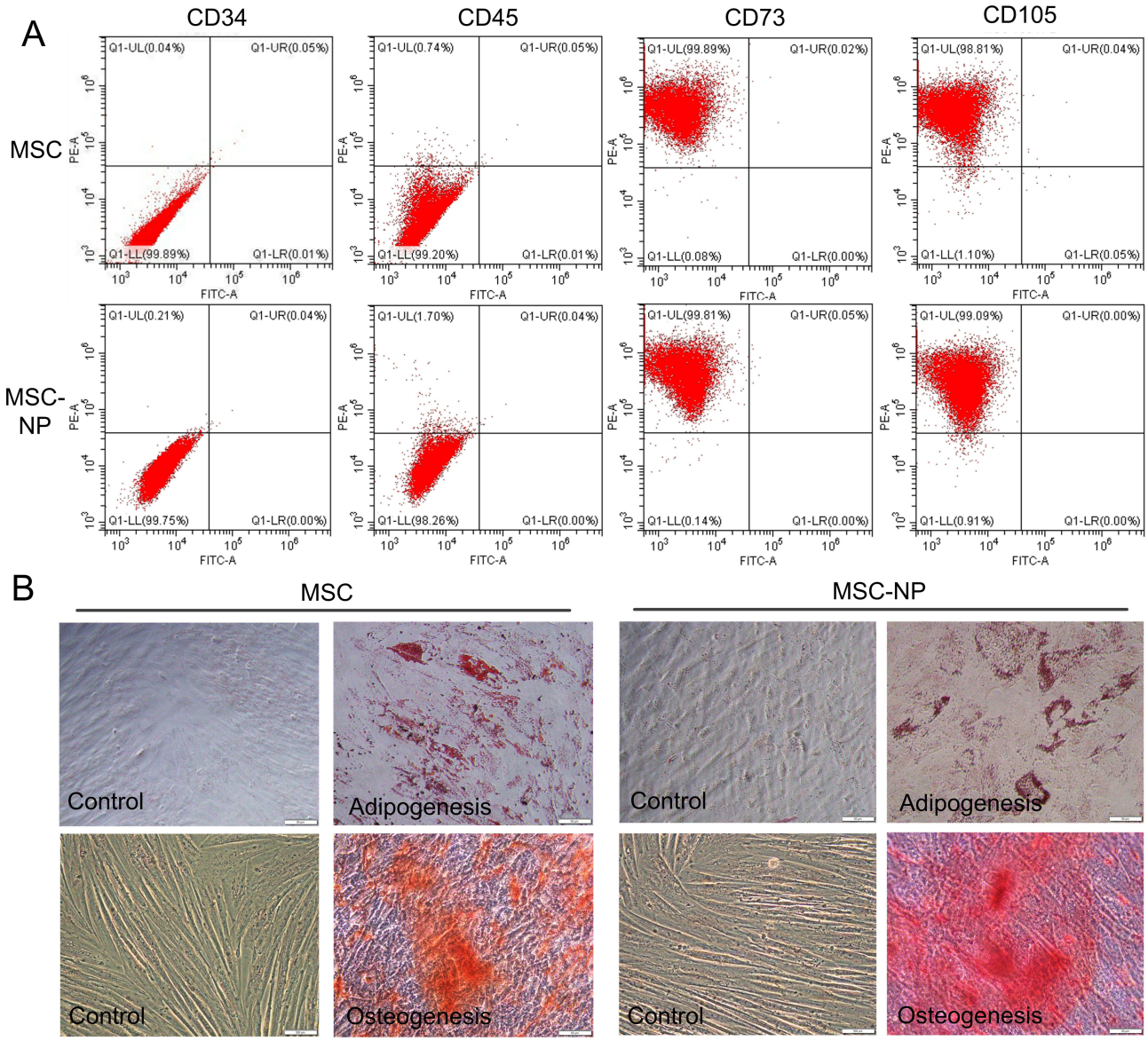

Figure 3 Fundamental Characteristics of Nanoparticle (NP)-Labeled Placental Mesenchymal Stem Cells (PL-MSCs). (**A**) Immunophenotyping of MSCs labeled with NPs compared to unlabeled MSCs. (**B**) Differentiation potential of MSCs into adipogenic and osteogenic lineages under various culture conditions.

MSCs alone. Furthermore, body weight, which significantly decreased in the DN group relative to the normal group, showed improvement after PL-MSC treatment (Figure 4B). The weight improvement was more significant in the magnetic targeted PL-MSC treatment group compared to the PL-MSC-treated group alone.

These findings indicate that magnetically targeted PL-MSCs effectively improve renal functional parameters in mice with DN, suggesting a protective effect on renal function. Previous studies have demonstrated that transplantation of bone marrow or umbilical cord MSCs can reduce proteinuria, serum creatinine, serum urea nitrogen, and urinary creatinine in diabetic mice and rats.[8,28,29] Importantly, the renal protection afforded by PL-MSCs was not due to glycemic control, as intravenously administered MSCs did not affect elevated serum glucose levels in mice with DN. Blood glucose levels in the three MSC-treated groups remained unchanged compared to the DN group (Figure 4C). This outcome aligns with previous reports[11] and may be attributed to the delayed treatment with PL-MSCs, potentially missing the optimal window for repairing acute pancreatic inflammatory injury. If the pancreatic islets are irreversibly damaged, their insulin-secreting function cannot be restored through MSC transplantation.

H&E staining revealed glomerular hypertrophy in mice with DN (Figure 5A). Enhanced extracellular matrix deposition was noted in the glomeruli and on the tubular basement membrane. Additionally, glomeruli exhibited thickened basement membranes and increased Bowman's space, as shown by PAS staining (Figure 5B). MT staining further identified glomerular and tubulointerstitial fibrosis in DN mouse kidneys (Figure 5C). However, treatment with PL-MSCs, both with and without NP labeling, alleviated these pathological changes. Notably, the group treated with magnetically targeted MSCs showed significantly improved pathological abnormalities compared to the non-targeted MSC-treated group.

TEM examination of the glomerulus revealed the ultrastructure of renal tissue. In the normal group, the glomerular filtration barrier comprised thin, fenestrated endothelial cells, regular glomerular basement membranes, and podocyte foot processes. The DN group exhibited diffuse thickening of the glomerular basement membrane and extensive foot

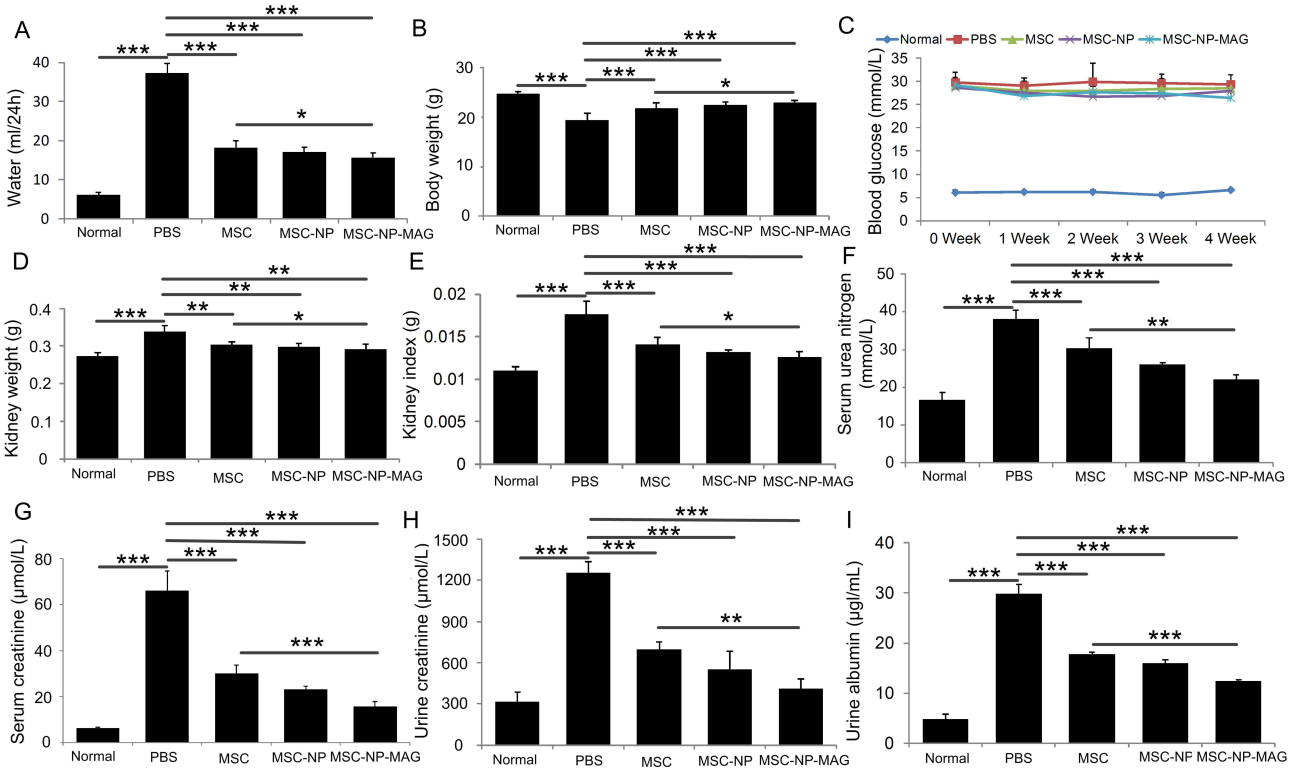

Figure 4 Comparative Effects of NP-Labeled and Unlabeled Placental Mesenchymal Stem Cell (PL-MSC) Treatments on Biochemical Indices in Mice with Diabetic Nephropathy (DN). (**A**) 24-hour water intake (n=5), (**B**) Body weight (n=5), (**C**) Blood glucose concentration curve (n=5), (**D**) Kidney weight (n=5), (**E**) Kidney index (n=5), (**F**) Serum urea nitrogen (n=5), (**G**) Serum creatinine (n=5), (**H**) Urine creatinine (n=5), and (**I**) Urinary albumin (n=5). Data are presented as mean ± S.E.M. *P*-values < 0.05 were considered statistically significant, denoted as **P* < 0.05; ***P* < 0.01; ****P* < 0.001.

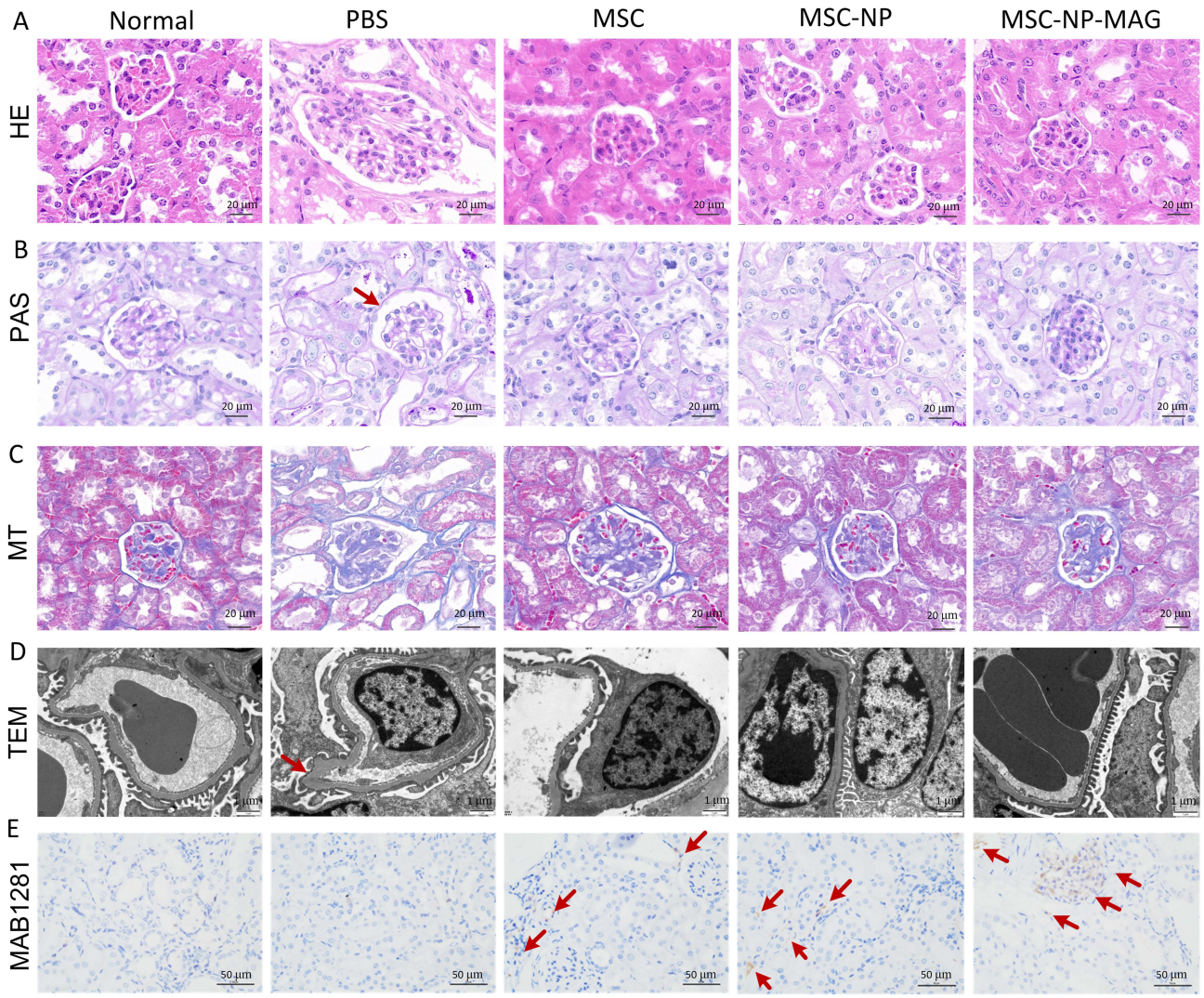

Figure 5 Histopathological Analysis of Tissues from Mice with Diabetic Nephropathy (DN). (**A**) Hematoxylin and Eosin (H&E) staining. (**B**) Periodic Acid-Schiff (PAS) staining. The red arrow indicates Bowman's space. (**C**) Masson's Trichrome staining. (**D**) Transmission Electron Microscopy (TEM) of renal tissues. The red arrow indicates thickening of the glomerular basement membrane. (**E**) Identification and distribution of Placental Mesenchymal Stem Cells (PL-MSCs) in the kidneys of mice with DN. The red arrow indicates MAB1281-positive cells in the kidney tissue.

process fusion and loss. In contrast, the MSC-treated group, particularly the magnetically targeted group, showed thin, regular glomerular basement membranes and intact podocyte foot processes (Figure 5D). Studies indicate that podocyte damage and loss, often due to prolonged high-glucose exposure, lead to renal dysfunction and proteinuria.[30–32] Our results suggest that magnetic targeting of MSCs can mitigate podocyte fusion and detachment, thereby preserving renal function and slowing DN progression.

Immunohistochemical staining for MAB1281 was used to identify PL-MSCs in mouse kidneys one week post-transplantation. In MSC-treated groups, few MAB1281-positive cells with brown nuclei were present in the kidneys. However, a larger number of MAB1281-positive cells were observed in the magnetically targeted MSC-treated group, primarily localized in the glomeruli. No MAB1281-positive cells were detected in the normal or DN groups (Figure 5E). This suggests that effective MSC homing to injured tissues is vital for successful treatment. Typically, MSCs are administered intravenously, which may lead to low uptake at the injury site. Some studies report significant MSC implantation in damaged tissues,[10,11,33,34] while others indicate that intravenous administration does not efficiently target MSCs to injured organs.[35] Furthermore, arterial MSC injection has been explored for immune regulation in kidney transplantation, but MSCs often accumulate in lung capillaries, resulting in insufficient targeting to injured tissue.[36]

These findings demonstrate that magnetic guidance significantly enhances MSC migration compared to non-magnetically guided MSCs.

Traditionally, DN has not been classified as an inflammatory disease. Yet, recent studies highlight the significant role of inflammatory responses in its pathogenesis.[37] Additionally, there is growing evidence that inflammation is key in initiating and progressing DN.[38,39] Among the therapeutic properties of MSCs, their anti-inflammatory efficacy is particularly notable. In our study, the DN group exhibited higher serum levels of pro-inflammatory cytokines, such as IL-1β, IL-2, IL-6, IL-12, IFN-γ, and TNF-α (Figure 6A), along with increased mRNA expression levels in kidney tissue (Figure 6B), compared to the normal group. These levels were significantly reduced after PL-MSC treatment, with a more pronounced decrease in the group treated with magnetically targeted MSCs. Notably, the mRNA expression levels of IL-2, IL-6, IFN-γ, and TNF-α were considerably lower in the magnetically targeted MSC-treated group than in the PL-MSC-treated group. The magnetic targeting enhanced the precise homing of injected PL-MSCs to the kidney tissues, thereby significantly boosting their anti-inflammatory capabilities. Consequently, the mRNA expression of inflammatory factors in the renal tissue of the magnetically targeted MSC group was substantially reduced, inhibiting the inflammatory response. These findings align with other studies that identified inflammation as a potential therapeutic target, noting that decreased inflammation improves kidney function.[8,40] Thus, magnetic targeting of MSCs effectively suppresses systemic and renal inflammation, improving diabetic kidney function by decreasing serum and kidney pro-inflammatory factors and increasing anti-inflammatory factors.

The accumulation of inflammatory cells in the kidneys is strongly linked to DN.[41,42] Additionally, the inhibition of inflammatory cell recruitment to the kidneys has been shown to protect against experimental DN.[43] Monocytes and

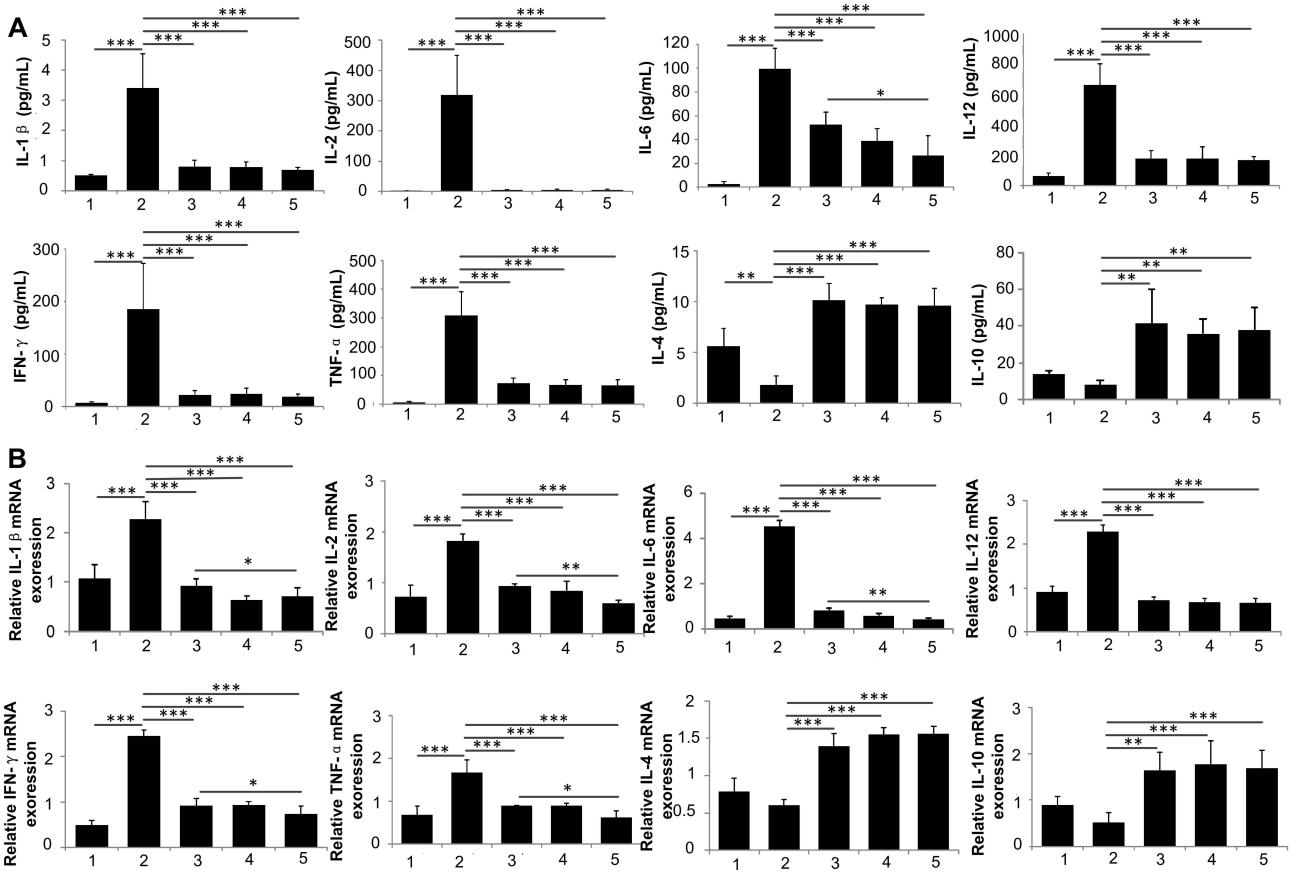

Figure 6 Impact of Mesenchymal Stem Cells (MSCs) on Inflammatory Cytokines in Mice with Diabetic Nephropathy (DN). (**A**) Temporal profile of cytokine levels in the serum of DN mice treated with phosphate-buffered saline (PBS), MSCs, nanoparticle (NP)-labeled MSCs, or magnetically targeted PL-MSCs (n=5). (**B**) Relative mRNA expression of inflammatory cytokines in kidney tissues (n=4). Data are presented as mean ± S.E.M. *P*-values < 0.05 were considered statistically significant, indicated as follows: **P* < 0.05; ***P* < 0.01; ****P* < 0.001.

macrophages are implicated in the pathogenesis of DN, and elevated levels of inflammatory biomarkers are indicative of an increased risk for DN.[44] MSCs effectively regulate the migration and filtration of immune cells, thereby mitigating inflammatory activation. In our study, the administration of PL-MSCs in mice with DN significantly reduced the recruitment of $Ly6G^+$ neutrophils (Figure 7A), $CD3^+$ lymphocytes (Figure 7B), and $F4/80^+$ macrophages (Figure 7C) to the kidney tissue. This reduction in inflammatory cell infiltration was confirmed by immunofluorescence staining, illustrating a decrease in the overall inflammatory response. Notably, treatment with magnetically targeted MSCs resulted in even less infiltration of inflammatory cells compared to other MSC treatments. Current research underscores the pivotal role of macrophages in the inflammatory process.[45,46] A variety of cytokines and chemokines released by macrophages, lymphocytes, and kidney cells activate the inflammatory signaling pathways in macrophages, contributing to the pathogenesis and progression of DN.[47] Macrophages secrete numerous cytokines, including pro-inflammatory cytokines such as TNF-α, IL-1β, IL-6, and IL-12, as well as various chemokines. Consequently, MSCs improve renal function in mice with DN by inhibiting the infiltration of inflammatory cells and the expression of inflammatory factors in renal tissue, thereby attenuating the inflammatory response.

To further explore the role of PL-MSCs in renal fibrosis, we analyzed molecular indicators of this condition. Immunofluorescence staining revealed that Collagen IV expression was predominantly found in the kidneys of the DN group; however, this expression significantly decreased in the PL-MSC-treated group, particularly in those receiving magnetically targeted MSC treatment (Figure 8A). Additionally, immunohistochemistry staining indicated elevated expressions of α-SMA and TGF-β in the DN group's kidneys, which were reduced following PL-MSC treatment, especially with magnetically targeted MSCs (Figure 8B and 8C). These findings suggest that Collagen IV, α-SMA, and TGF-β levels in the kidneys of DN mice decreased following MSC treatment, paralleling a reduction in inflammatory factors. Notably, MSC treatment often concurrently diminishes fibrosis and inflammatory responses, potentially due to overlapping pathways in fibrosis and inflammation.

Macrophages, the primary cellular source of TGF-β, disrupt cell cycle progression and contribute to renal hypertrophy in early-stage DN. TGF-β is recognized as a key factor in inducing fibrosis during the chronic stages of various organ and tissue inflammatory diseases. The TGF-β pathway facilitates the differentiation of fibroblasts into myofibroblasts, associated with the transdifferentiation of renal tubular epithelial cells into fibroblasts, leading to renal interstitial fibrosis.[48] qPCR and ELISA confirmed that TGF-β contributes to renal fibrosis (Figure 8D) and that serum cytokine levels of TGF-β were significantly higher in the DN group compared to the normal group. However, treatment with magnetically targeted PL-MSCs markedly suppressed this increase, correlating with enhanced MSC aggregation in the

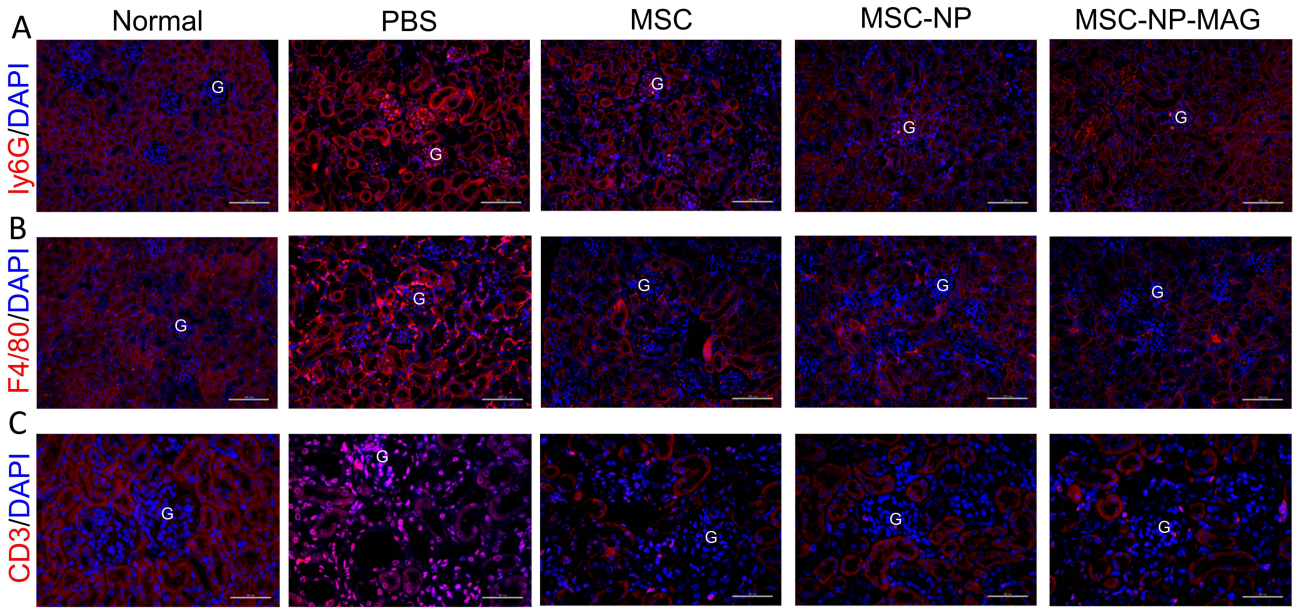

Figure 7 Inflammation in Kidneys of Mice with Diabetic Nephropathy (DN). Immunofluorescence staining is used to identify Ly6G+ neutrophils (**A**), Scale bar = 100 μm), F4/80+ macrophages (**B**), Scale bar = 100 μm), and CD3+ lymphocytes (**C**), Scale bar = 50 μm) in kidney tissue sections. "G" denotes the glomerulus.

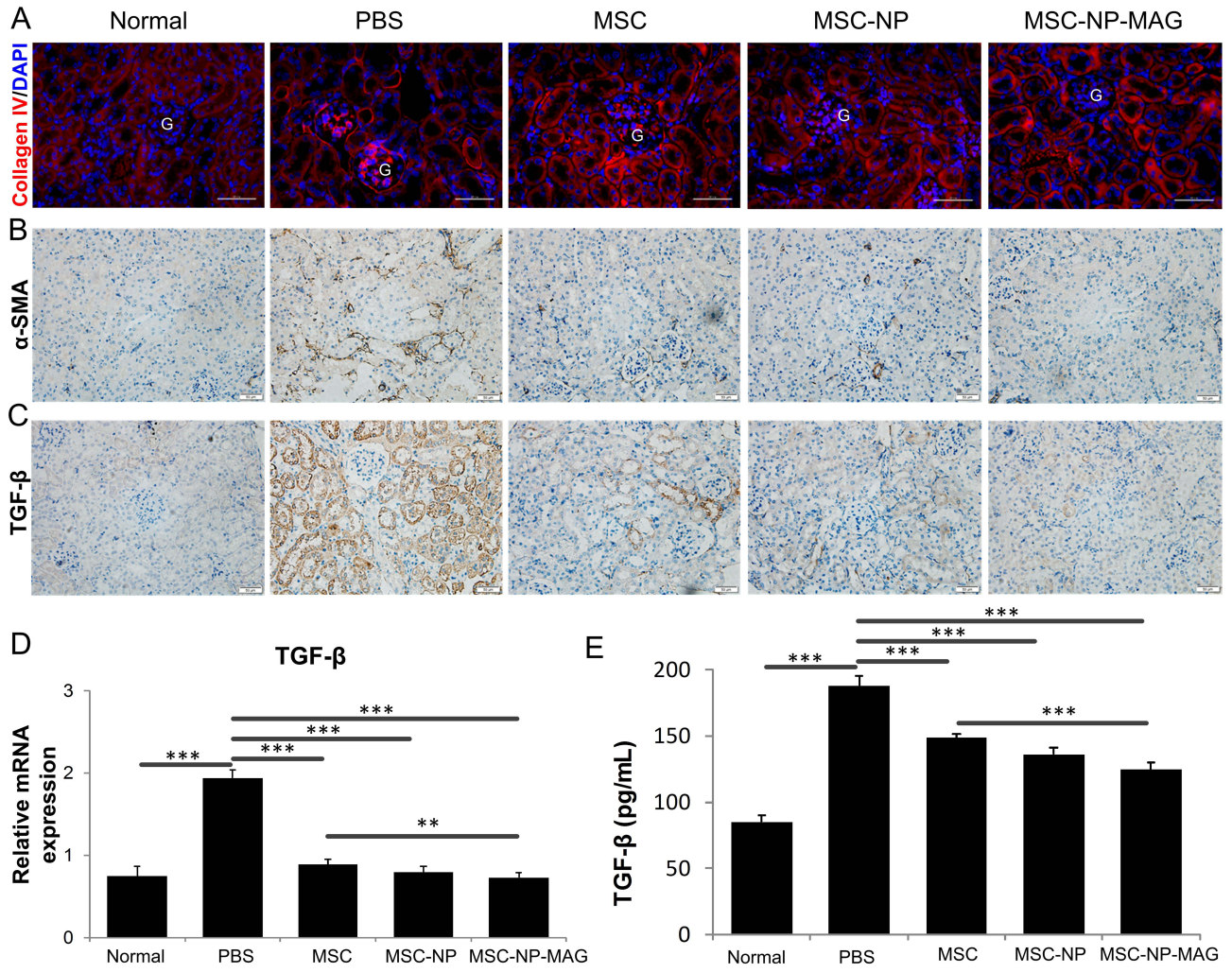

Figure 8 Impact of Nanoparticle (NP)-Labeled and Unlabeled Mesenchymal Stem Cell (MSC) Treatments on Kidney Fibrosis in Mice with Diabetic Nephropathy (DN). (**A**) Immunohistochemistry staining for (**B**) α-smooth muscle actin and (**C**) transforming growth factor-β (TGF-β) in kidney tissues. (**D**) Quantitative analysis of TGF-β mRNA expression in kidney tissues (n=4). (**E**) Plasma levels of TGF-β (n=5). Data are represented as mean ± S.E.M. *P*-values < 0.05 were considered statistically significant, indicated as $^{**}P < 0.01$; $^{***}P < 0.001$.

kidneys due to magnetic targeting. This suggests that inhibiting TGF-β expression is a potential mechanism behind the anti-fibrotic effects of magnetically targeted PL-MSCs.

Magnetically targeted PL-MSCs significantly reduced the expression of TGF-β and diminished the presence of fibroblast markers, such as collagen IV and α-SMA, in the kidneys of mice with DN. Immunofluorescence staining revealed that the infusion of magnetically targeted MSCs mitigated renal fibrosis in DN mice, aligning with previous research on the impact of MSCs derived from various tissues on kidney fibrosis.[8,49] The augmented effect of magnetically targeting MSCs on renal fibrosis in DN mice may be intricately linked to the TGF-β signaling pathway. In conclusion, our findings indicate that decreasing these fibrotic and inflammatory factors in the kidneys affected by DN can enhance renal function. This contributes to a more comprehensive understanding of how magnetically targeted MSCs assist in restoring kidney function in DN.

Conclusion

In summary, our study presents the approach in regenerative cell therapy by imparting magnetic properties to PL-MSCs using Fe_3O_4@PDA NP labeling. This technique, coupled with the use of external magnets, significantly enhances the concentration of NP-labeled MSCs at targeted sites through intravenous injection. A key advantage of this method is its

non-toxic nature, which importantly does not compromise the essential characteristics of PL-MSCs. The research highlights the effectiveness of magnetic targeting in directing NP-labeled MSCs to the kidney area in DN models. This targeting capability was shown to be instrumental in reducing albuminuria and glomerular injury, thus improving renal function more efficiently than treatments with non-guided MSCs or NP-labeled MSCs without magnetic guidance. The enhanced homing ability fostered by magnetic targeting also contributed to a decrease in fibrosis and inflammation, amplifying the therapeutic impact of PL-MSCs in DN.

Data Sharing Statement

All data generated or analyzed during this study are included in this publication.

Funding

This study was funded by the National Natural Science Foundation of China (Grant No. 82000765), the Education Department of Jilin Province (Grant No. JJKH20211148KJ), the Spring Bud Project of the China-Japan Union Hospital of Jilin University (Grant No. 2023CL03, 2023CL02, 2023CL06), and Science and Technology Department of Jilin Province (No. YDZJ202201ZYTS241, 20220203120SF).

Disclosure

Ke Wang and Te Liu contributed equally to this work and are co-first authors. The authors declare no conflicts of interest in relation to this work.

References

1. Ali MK, Pearson-Stuttard J, Selvin E, et al. Interpreting global trends in type 2 diabetes complications and mortality. *Diabetologia*. 2022;65(1):3–13. doi:10.1007/s00125-021-05585-2
2. Crandall JP, Knowler WC, Kahn SE, et al. The prevention of type 2 diabetes. *Nat Clin Pract Endocrinol Metab*. 2008;4(7):382–393. doi:10.1038/ncpendmet0843
3. Golden SH. Emerging therapeutic approaches for the management of diabetes mellitus and macrovascular complications. *Am J Cardiol*. 2011;108(3 Suppl):59b–67b. doi:10.1016/j.amjcard.2011.03.017
4. Molitch ME. Nephropathy in diabetes. *Diabetes Care*. 2004;27(Suppl 1):S79–83.
5. Espinel E, Agraz I, Ibernon M, et al. Renal biopsy in type 2 diabetic patients. *J Clin Med*. 2015;4(5):998–1009. doi:10.3390/jcm4050998
6. Lebovitz HE. Thiazolidinediones: the forgotten diabetes medications. *Curr Diab Rep*. 2019;19(12):151. doi:10.1007/s11892-019-1270-y
7. Tögel F, Westenfelder C. Adult bone marrow-derived stem cells for organ regeneration and repair. *Dev Dyn*. 2007;236(12):3321–3331. doi:10.1002/dvdy.21258
8. Xiang E, Han B, Zhang Q, et al. Human umbilical cord-derived mesenchymal stem cells prevent the progression of early diabetic nephropathy through inhibiting inflammation and fibrosis. *Stem Cell Res Ther*. 2020;11(1):336. doi:10.1186/s13287-020-01852-y
9. Lee SE, Chathuranga K, Lee J-S, et al. Mesenchymal stem cells prevent the progression of diabetic nephropathy by improving mitochondrial function in tubular epithelial cells. *Exp Mol Med*. 2019;51(7):1–14. doi:10.1038/s12276-019-0299-y
10. Ezquer F, Ezquer M, Simon V, et al. Endovenous administration of bone-marrow-derived multipotent mesenchymal stromal cells prevents renal failure in diabetic mice. *Biol Blood Marrow Transplant*. 2009;15(11):1354–1365. doi:10.1016/j.bbmt.2009.07.022
11. Wang S, Li Y, Zhao J, et al. Mesenchymal stem cells ameliorate podocyte injury and proteinuria in a type 1 diabetic nephropathy rat model. *Biol Blood Marrow Transplant*. 2013;19(4):538–546. doi:10.1016/j.bbmt.2013.01.001
12. Zhang L, Li K, Liu X, et al. Repeated systemic administration of human adipose-derived stem cells attenuates overt diabetic nephropathy in rats. *Stem Cells Dev*. 2013;22(23):3074–3086. doi:10.1089/scd.2013.0142
13. Li X, Bai J, Ji X, et al. Comprehensive characterization of four different populations of human mesenchymal stem cells as regards their immune properties, proliferation and differentiation. *Int J Mol Med*. 2014;34(3):695–704. doi:10.3892/ijmm.2014.1821
14. Li X, Wei Z, Wu L, et al. Efficacy of Fe 3 O 4 @polydopamine nanoparticle-labeled human umbilical cord Wharton's jelly-derived mesenchymal stem cells in the treatment of streptozotocin-induced diabetes in rats. *Biomater Sci*. 2020;8(19):5362–5375. doi:10.1039/D0BM01076F
15. Hour FQ, Moghadam AJ, Shakeri-Zadeh A, et al. Magnetic targeted delivery of the SPIONs-labeled mesenchymal stem cells derived from human wharton's jelly in alzheimer's rat models. *J Control Release*. 2020;321:430–441. doi:10.1016/j.jconrel.2020.02.035
16. Chaudeurge A, Wilhelm C, Chen-Tournoux A, et al. Can magnetic targeting of magnetically labeled circulating cells optimize intramyocardial cell retention? *Cell Transplant*. 2012;21(4):679–691. doi:10.3727/096368911X612440
17. Saldanha KJ, Doan RP, Ainslie KM, et al. Micrometer-sized iron oxide particle labeling of mesenchymal stem cells for magnetic resonance imaging-based monitoring of cartilage tissue engineering. *Magn Reson Imaging*. 2011;29(1):40–49. doi:10.1016/j.mri.2010.07.015
18. Hill JM, Dick AJ, Raman VK, et al. Serial cardiac magnetic resonance imaging of injected mesenchymal stem cells. *Circulation*. 2003;108(8):1009–1014. doi:10.1161/01.CIR.0000084537.66419.7A
19. Ma R, He Y, Fang Q, et al. Ferulic acid ameliorates renal injury via improving autophagy to inhibit inflammation in diabetic nephropathy mice. *Biomed Pharmacother*. 2022;153:113424. doi:10.1016/j.biopha.2022.113424
20. Garzón I, Pérez-Köhler B, Garrido-Gómez J, et al. Evaluation of the cell viability of human Wharton's jelly stem cells for use in cell therapy. *Tissue Eng Part C Methods*. 2012;18(6):408–419. doi:10.1089/ten.tec.2011.0508

21. Rodriguez-Morata A, Garzon I, Alaminos M, et al. Cell viability and prostacyclin release in cultured human umbilical vein endothelial cells. *Ann Vasc Surg*. 2008;22(3):440–448. doi:10.1016/j.avsg.2008.03.004
22. González-Andrades M, Garzón I, Gascón MI, et al. Sequential development of intercellular junctions in bioengineered human corneas. *J Tissue Eng Regen Med*. 2009;3(6):442–449. doi:10.1002/term.178
23. Kim SJ, Lewis B, Steiner MS, et al. Superparamagnetic iron oxide nanoparticles for direct labeling of stem cells and in vivo MRI tracking. *Contrast Media Mol Imaging*. 2016;11(1):55–64. doi:10.1002/cmmi.1658
24. Soenen SJ, De Cuyper M. Assessing cytotoxicity of (iron oxide-based) nanoparticles: an overview of different methods exemplified with cationic magnetoliposomes. *Contrast Media Mol Imaging*. 2009;4(5):207–219. doi:10.1002/cmmi.282
25. Dominici M. Minimal criteria for defining multipotent mesenchymal stromal cells. *Int Soc Cell Therapy Position State Cytoth*. 2006;8(4):315–317.
26. Nombela-Arrieta C, Ritz J, Silberstein LE. The elusive nature and function of mesenchymal stem cells. *Nat Rev Mol Cell Biol*. 2011;12(2):126–131. doi:10.1038/nrm3049
27. Uccelli A, Moretta L, Pistoia V. Mesenchymal stem cells in health and disease. *Nat Rev Immunol*. 2008;8(9):726–736. doi:10.1038/nri2395
28. Ezquer FE, Ezquer ME, Parrau DB, et al. Systemic administration of multipotent mesenchymal stromal cells reverts hyperglycemia and prevents nephropathy in type 1 diabetic mice. *Biol Blood Marrow Transplant*. 2008;14(6):631–640. doi:10.1016/j.bbmt.2008.01.006
29. Li H, Rong P, Ma X, et al. Mouse umbilical cord mesenchymal stem cell paracrine alleviates renal fibrosis in diabetic nephropathy by reducing myofibroblast transdifferentiation and cell proliferation and upregulating mmps in mesangial cells. *J Diabetes Res*. 2020;2020:3847171. doi:10.1155/2020/3847171
30. Isermann B, Vinnikov IA, Madhusudhan T, et al. Activated protein C protects against diabetic nephropathy by inhibiting endothelial and podocyte apoptosis. *Nat Med*. 2007;13(11):1349–1358. doi:10.1038/nm1667
31. Jha JC, Thallas-Bonke V, Banal C, et al. Podocyte-specific Nox4 deletion affords renoprotection in a mouse model of diabetic nephropathy. *Diabetologia*. 2016;59(2):379–389. doi:10.1007/s00125-015-3796-0
32. Dalla Vestra M, Masiero A, Roiter AM, et al. Is podocyte injury relevant in diabetic nephropathy? Studies in patients with type 2 diabetes. *Diabetes*. 2003;52(4):1031–1035. doi:10.2337/diabetes.52.4.1031
33. Semedo P, Correa-Costa M, Antonio Cenedeze M, et al. Mesenchymal stem cells attenuate renal fibrosis through immune modulation and remodeling properties in a rat remnant kidney model. *Stem Cells*. 2009;27(12):3063–3073. doi:10.1002/stem.214
34. Mouiseddine M. Intravenous human mesenchymal stem cells transplantation in NOD/SCID mice preserve liver integrity of irradiation damage. *Methods Mol Biol*. 2012;826:179–188.
35. Schrepfer S, Deuse T, Reichenspurner H, et al. Stem cell transplantation: the lung barrier. *Transplant Proc*. 2007;39(2):573–576. doi:10.1016/j.transproceed.2006.12.019
36. Zonta S, De Martino M, Bedino G, et al. Which is the most suitable and effective route of administration for mesenchymal stem cell-based immunomodulation therapy in experimental kidney transplantation: endovenous or arterial? *Transplant Proc*. 2010;42(4):1336–1340. doi:10.1016/j.transproceed.2010.03.081
37. Donate-Correa J, Luis-Rodríguez D, Martín-Núñez E, et al. Inflammatory targets in diabetic nephropathy. *J Clin Med*. 2020;9(2):458. doi:10.3390/jcm9020458
38. Navarro JF, Mora C. Role of inflammation in diabetic complications. *Nephrol Dial Transplant*. 2005;20(12):2601–2604. doi:10.1093/ndt/gfi155
39. Wong CK, Ho AWY, Tong PCY, et al. Aberrant activation profile of cytokines and mitogen-activated protein kinases in type 2 diabetic patients with nephropathy. *Clin Exp Immunol*. 2007;149(1):123–131. doi:10.1111/j.1365-2249.2007.03389.x
40. Walther CP, Navaneethan SD. Inflammation as a therapeutic target to improve vascular function in kidney disease. *J Am Soc Nephrol*. 2017;28(3):723–725. doi:10.1681/ASN.2016111173
41. Calle P, Hotter G. Macrophage phenotype and fibrosis in diabetic nephropathy. *Int J Mol Sci*. 2020;21(8):2806. doi:10.3390/ijms21082806
42. Nguyen D, Ping FU, Mu W, et al. Macrophage accumulation in human progressive diabetic nephropathy. *Nephrology*. 2006;11(3):226–231. doi:10.1111/j.1440-1797.2006.00576.x
43. Awad AS, Kinsey GR, Khutsishvili K, et al. Monocyte/macrophage chemokine receptor CCR2 mediates diabetic renal injury. *Am J Physiol Renal Physiol*. 2011;301(6):F1358–66. doi:10.1152/ajprenal.00332.2011
44. Huang M, Zhu Z, Nong C, et al. Bioinformatics analysis identifies diagnostic biomarkers and their correlation with immune infiltration in diabetic nephropathy. *Ann Transl Med*. 2022;10(12):669. doi:10.21037/atm-22-1682
45. Zhang Y, Le X, Zheng S, et al. MicroRNA-146a-5p-modified human umbilical cord mesenchymal stem cells enhance protection against diabetic nephropathy in rats through facilitating M2 macrophage polarization. *Stem Cell Res Ther*. 2022;13(1):171. doi:10.1186/s13287-022-02855-7
46. Zheng S, Zhang K, Zhang Y, et al. Human umbilical cord mesenchymal stem cells inhibit pyroptosis of renal tubular epithelial cells through mir-342-3p/caspase 1 signaling pathway in diabetic nephropathy. *Stem Cells Int*. 2023;2023:5584894. doi:10.1155/2023/5584894
47. Shao BY, Zhang S-F, Li H-D, et al. Epigenetics and inflammation in diabetic nephropathy. *Front Physiol*. 2021;12:649587. doi:10.3389/fphys.2021.649587
48. Ina K, Kitamura H, Tatsukawa S, et al. Transformation of interstitial fibroblasts and tubulointerstitial fibrosis in diabetic nephropathy. *Med Electron Microsc*. 2002;35(2):87–95. doi:10.1007/s007950200011
49. An X, Liao G, Chen Y, et al. Intervention for early diabetic nephropathy by mesenchymal stem cells in a preclinical nonhuman primate model. *Stem Cell Res Ther*. 2019;10(1):363. doi:10.1186/s13287-019-1401-z